

CNRS

*Centre National de la Recherche Scientifique*

INFN

*Istituto Nazionale di Fisica Nucleare*



# Conceptual design of AdvancedVirgo photon calibration

L. Rolland, F. Marion, B. Mours

**VIR-0013A-15**

February 4, 2015

VIRGO \* A joint CNRS-INFN Project

Project office: Traversa H di via Macerata - I-56021 S. Stefano a Macerata, Cascina (PI)  
Secretariat: Telephone (39) 50 752 521 – Fax (39) 50 752 550 – e-mail [virgo@pisa.infn.it](mailto:virgo@pisa.infn.it)

# Contents

<b>1</b>	<b>Introduction</b>	<b>4</b>
<b>2</b>	<b>The PCal used in Virgo</b>	<b>4</b>
<b>3</b>	<b>Goals and general design of the AdV PCal</b>	<b>5</b>
3.1	Verification of the sign of $h(t)$ . . . . .	6
3.2	Cross-check of the standard actuator calibration and $h(t)$ reconstruction . . . . .	6
3.3	Monitoring of the calibration stability . . . . .	7
3.4	Hardware and blind injections . . . . .	7
<b>4</b>	<b>Excitation of the mirror internal modes</b>	<b>7</b>
<b>5</b>	<b>Interface with other sub-systems</b>	<b>8</b>
5.1	PCal locations and optical benches (VAC) . . . . .	8
5.2	Positions of the end mirrors, windows and benches for the PCal (VAC, SAT, PAY, INF) . . . . .	10
5.3	Viewports for the PCal (VAC) . . . . .	10
5.4	Mass of the end mirror (MIR, PAY) . . . . .	10
5.5	Payloads and baffles (PAY, SLC) . . . . .	11
5.6	Position of the main ITF beam on the end mirror (ISC) . . . . .	11
<b>6</b>	<b>Some constraints on the PCal design</b>	<b>11</b>
6.1	Laser wavelength and polarization . . . . .	11
6.2	Minimum laser power . . . . .	12
6.2.1	Permanent lines . . . . .	12
6.2.2	Calibration up to 1 kHz . . . . .	13
6.2.3	Hardware injections . . . . .	13
6.2.4	Conclusion . . . . .	16
6.3	Power noise . . . . .	17
6.4	Laser beam profile . . . . .	18
6.5	Alignment of main and PCal beams on the mirror . . . . .	18
6.6	Power calibration and choice of the powermeter . . . . .	20
6.7	Timing synchronization and timing calibration . . . . .	21
<b>7</b>	<b>Possible ideas</b>	<b>21</b>
<b>8</b>	<b>Summary</b>	<b>22</b>
<b>A</b>	<b>Optocad simulations to select the windows for the PCal</b>	<b>25</b>
A.1	Single beam PCal configuration . . . . .	25
A.2	Two-beam PCal configuration . . . . .	26

---

<b>B</b>	<b>AdV reference sensitivity curves</b>	<b>29</b>
<b>C</b>	<b>Details about hardware injections</b>	<b>30</b>
C.1	BNS signal simulation: generation script using lalsuite . . . . .	30
C.2	BNS signal simulation: terminal output . . . . .	30
C.3	Configuration file of HInjection process . . . . .	31
C.4	Some more plots . . . . .	31

# 1 Introduction

The photon calibrator (PCal) is a mirror actuator that uses the radiation pressure of an auxiliary laser to act on the mirror. It is independent from the electromagnetic actuators used to control the mirrors of the interferometer (ITF).

The PCal is mainly used for ITF calibration purpose. It has been installed in Virgo and used as a check of the standard calibration during the Virgo Science Runs VSR1 to VSR4 [1, 2, 3, 4, 5]. PCal setups have also been used in the GEO and LIGO detectors [6, 8].

The goals of the photon calibration for Advanced Virgo are summarized in this document. The interfaces with the other AdV sub-systems are then highlighted. Finally, the main constraints to be taken into account in the PCal design are detailed.

## 2 The PCal used in Virgo

During Virgo, the PCal setup was installed around the NI mirror, with a single beam hitting the center of the mirror. It could induce mirror displacements of the order of  $6 \times 10^{-15}$  m at 10 Hz.

It has been mainly used to check the sign of the reconstructed gravitational wave (GW) strain signal  $h(t)$  and to check the amplitude and phase of the reconstructed  $h(t)$  signal in the band 10 Hz to 5 kHz.

A parallel way to analyze the PCal data could have been to extract calibration of the electromagnetic actuators comparing the amplitude of the lines sent via the two types of actuators in the dark fringe signal. This has not been performed extensively.

The uncertainties on the mirror displacement applied to the mirror by the PCal were of the order of 7% in amplitude and  $< 10 \mu\text{s}$  in timing. The details of the calibration of the PCal during VSR3 and VSR4 are described in [4, 5].

Sine motions of the NI mirror up to 6 kHz were induced with the PCal during VSR4. The PCal beam hitting the center of the mirror, it was strongly coupled to the drum modes of the mirror. As a consequence, the mirror did not behaved as a rigid body above few hundreds of hertz as already shown in GEO [7]. However, a model for the coupling of the PCal beam with the internal modes of the mirror has been extracted from the data measured at high frequency: as shown in figure 1, the sum of the contributions of the different mirror mechanical modes (mainly pendulum and drum mode in this case), modifies the pendulum response. In particular, the contribution of the drum modes induces a notch, which for Virgo NI mirror, was measured close to 2100 Hz. This analysis allowed to validate the reconstructed  $h(t)$  channel up to 6 kHz with the PCal [4, 5].

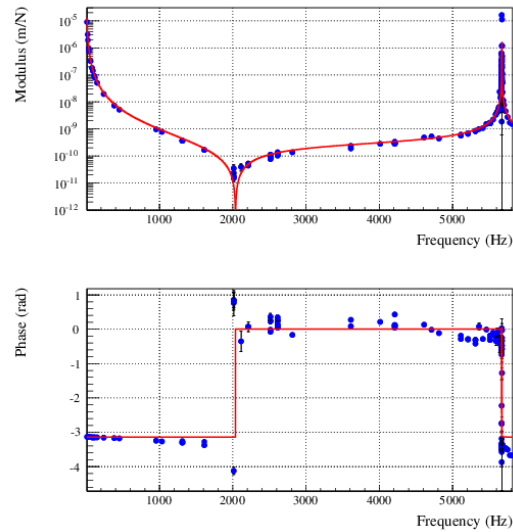


Figure 1: Mechanical response: mirror motion sensed by the ITF when a force was applied with the Virgo PCal during VSR4. Blue points: measurements made with the PCal during VSR4. Red line: model of the mechanical transfer function. The  $1/f^2$  pendulum response dominates at low frequency, with a phase of  $-\pi$  with respect to the force. The response of the drum mode is a second-order low-pass filter, whose resonance is visible a bit above 5.6 kHz ; it is in-phase with the force below the resonance frequency. The full response being the sum of the contributions from the different modes, they cancel at some frequency, inducing a notch around 2.1 kHz.

### 3 Goals and general design of the AdV PCal

The main goals of the PCal are:

- a direct verification of the sign of the reconstructed  $h(t)$  channel,
- a cross-check of the standard electro-magnetic actuator calibration and  $h(t)$  reconstruction,
- a permanent monitoring to assess the stability of the electro-magnetic actuators and of the  $h(t)$  reconstruction,
- if possible, a second way to perform hardware or blind injections of GW-like signals in the ITF.

Two PCal's are planned for AdV, one at each end mirror. This will allow to cross-check their absolute power calibration.

### 3.1 Verification of the sign of $h(t)$

The verification of the sign of the reconstructed  $h(t)$  channel can be done almost "directly", without any power calibration of the PCal setup. The data consist in inducing one sinusoidally-modulated displacement of the mirror below few tenths of hertz. The knowledge of the side of the mirror hit by the laser beam and the sign of the force with respect to the signal of the photodiode used to monitor the PCal beam is enough for this analysis.

### 3.2 Cross-check of the standard actuator calibration and $h(t)$ reconstruction

Ideally, the cross-check of the standard calibration is most efficient if the PCal calibration is as precise as the standard calibration. Requirements on the precision of the reconstructed amplitude and phase of  $h(t)$  for AdV are given by the data analysis groups [9, 10] to be below  $\sim 5\%$  in amplitude,  $\sim 5^\circ$  (90 mrad) and  $10 \mu s$  in phase and timing.

The AdV detector most sensitive range to GW signals is below few hundreds of hertz. In this range, the mirror behaves as a rigid body and this goal is realistic.

At higher frequencies, the mirror internal modes have to be taken into account, which might increase the uncertainties in the PCal calibration (see more details in section 4). To overcome this issue, GEO and LIGO have chosen to install PCal's with two beams hitting the mirrors at locations where the force coupling to the drum modes of the mirror is low. However, the analysis of VSR4 data has shown that the drum modes can be modeled from the data and taken into account properly, without increasing a lot the uncertainties on the PCal calibration at high frequency.

Moreover, in the case of a setup which do not excite the internal modes, applying excitation to the mirrors higher than  $\sim 1$  kHz is challenging due to the  $1/f^2$  mechanical response, while in the case the drum modes are excited, the mechanical model is flat after a notch at  $\sim 2$  kHz, which allow to have data at high frequencies. The details of the expected shape of the mechanical model with the drum modes has still to be studied.

Since the PCal setup and its power calibration would be much simpler with a single beam hitting the center of the mirror, the baseline design of the PCal for AdV will still have a single beam. However, in case problems arise from this setup, the possibility to upgrade it to two beams should be kept.

### 3.3 Monitoring of the calibration stability

Permanent calibration lines injected with the PCal, along with the lines injected via the electromagnetic actuators will be setup for AdV. They are useful to monitor the stability of the actuator calibration, and possibly highlight for any unexpected change in the actuation setup. They are also useful to monitor the sign of the reconstructed  $h(t)$  and the stability of the reconstruction as function of time.

### 3.4 Hardware and blind injections

As shown later in section 6.2.3, the PCal actuator can be used to simulate GW-like signals in the AdV detector, injecting the so-called hardware injections. In particular, it may be used for the blind injections since the PCal actuators are completely independent from the ITF control. In this case, one PCal can be used for permanent line injections, and the second PCal can be used for the hardware injections.

## 4 Excitation of the mirror internal modes

The amplitude of the mirror motion applied with the PCal beam power-modulated at frequency  $f$  is (assuming the mirror is a rigid body):

$$\Delta x_{rigid}(t) = -\frac{1}{m} \frac{1}{(2\pi f)^2} \times \Delta F(t) = -\frac{1}{m} \frac{2 \cos(i)}{c} \frac{\Delta P_{ref}(t)}{(2\pi f)^2} \quad (1)$$

where  $m$  is the mass of the mirror,  $F$  the applied force,  $i$  the angle of incidence of the beam on the mirror,  $P_{ref}$  the reflected power estimated from a calibrated photodiode.

However, it is unavoidable to excite some mirror internal modes when applying a force with the PCal. With a 1-beam PCal setup as used during Virgo+, the drum modes will be excited when applying a force with the PCal. To predict such an effect in the case of AdV, FEM simulations have been performed by PAY with the following logic:

1. first FEM simulations of the Virgo NI mirror have been carried out, assuming the PCal induces a point-like force on the mirror. They have shown that the mechanical response measured with the PCal and shown in figure 1 can be recovered by simulations when both a large enough number of internal modes and the size of the ITF beam that senses the displacement are taken into account. In particular, the notch measured around 2100 Hz was recovered by the simulations.
2. then FEM simulations of the AdV end mirrors have been carried out. Preliminary results show that a notch is expected around 2300 Hz. Its frequency could be increased a bit if the PCal beam would be miscentered on the mirror.

In the following sections, the power of the laser needed for some particular excitations is estimated. In this case, the mechanical response is assumed to be the sum of two transfer functions:

- the pendulum: a second order low-pass filter with  $f_p = 0.6$  Hz and  $Q = 1000$ .
- the drum mode(s): a second order low-pass filter with  $f_p = 7840$  Hz and  $Q = 60 \times 10^6$ , normalized such that the sum of the two transfer functions is zero at 2300 Hz. The properties of the drum mode and the frequency at which the sum gives zero are preliminary estimations of the AdV payload simulations.

In order to simulate such a response in the hardware injection software, it has been approximated by the product of the pendulum response and of a zero with  $f_0 = 2300$  Hz and  $Q = 100$ . Below 2000 Hz, this approximation agrees with the initial model within better than 6% in modulus, and 35 mrad (or  $3 \mu\text{s}$ ) in phase.

It is possible to reduce the excitation of the drum modes setting up a 2-beam PCal, with the 2 beams pushing on the mirror symmetrically around its center. In the ideal case where the internal mirror modes are not excited (i.e. the mirror can be considered as a rigid body), the response is only the one of the pendulum.

As discussed in section 3.2, the baseline for the AdV PCal is the single-beam setup, but the possibility to upgrade the setup to a 2-beam must be kept.

## 5 Interface with other sub-systems

The interfaces of the PCal setup with other AdV sub-systems are described in this section. The first items deal with general setup issues while other items deal with inputs needed to improve the absolute calibration of the PCal actuators.

The most important parameters to be known for the PCal calibration are highlighted in the equation 1.

### 5.1 PCal locations and optical benches (VAC)

For AdV, two PCal's will be installed, one around each end mirror, NE and WE. The PCal beam have to hit the mirror on the HR face from the interior of the arm Fabry-Perot cavity.

Two possibilities have been considered concerning the windows to install the setup. They are shown in the figure 2:

1. similar configuration as in Virgo (red circles): windows of diameter 136 mm, located  $\sim 1$  m from the end mirror, seeing the mirror with an incidence angle of  $\sim 42^\circ$ .



2. new configuration using new windows around the cryotrap (yellow circles): windows of diameter 63 mm, located horizontally  $\sim 1.5$  m from the end mirror, seeing the mirror with an incidence angle of  $\sim 17^\circ$ . The location of the windows is known within a few mm, better than 1 cm [18].

The systematic uncertainty on the PCal actuation coming from the uncertainty on the incidence angle of the PCal on the mirror is lower when the angle is lower. As a consequence, option 2 is more convenient. It has also the advantage to have horizontal optical benches, which must ease the installation and calibration procedures. The main drawback of option 2 is the reduced size of the windows' aperture. Optocad simulations of this configuration have been performed (see appendix A) and confirmed that a PCal beam reflected at the center of the mirror HR surface can be collected through the opposite viewport.

As a consequence, option 2 (new viewports around the cryotrap link) has been selected.

Two optical benches will be installed: one for the injection of the PCal beam, and one to get the beam reflected on the end mirror. The space for the optical benches around these windows is limited. Typical bench size could be  $25\text{ cm} \times 50\text{ cm}$  (the distance between the window and the cryotrap is 50 cm but some space must be left for "regeneration" procedure of the cryotrap). These benches will have to be designed and built at LAPP.

The injection bench will be more crowded than the reflection bench. On the side-view of

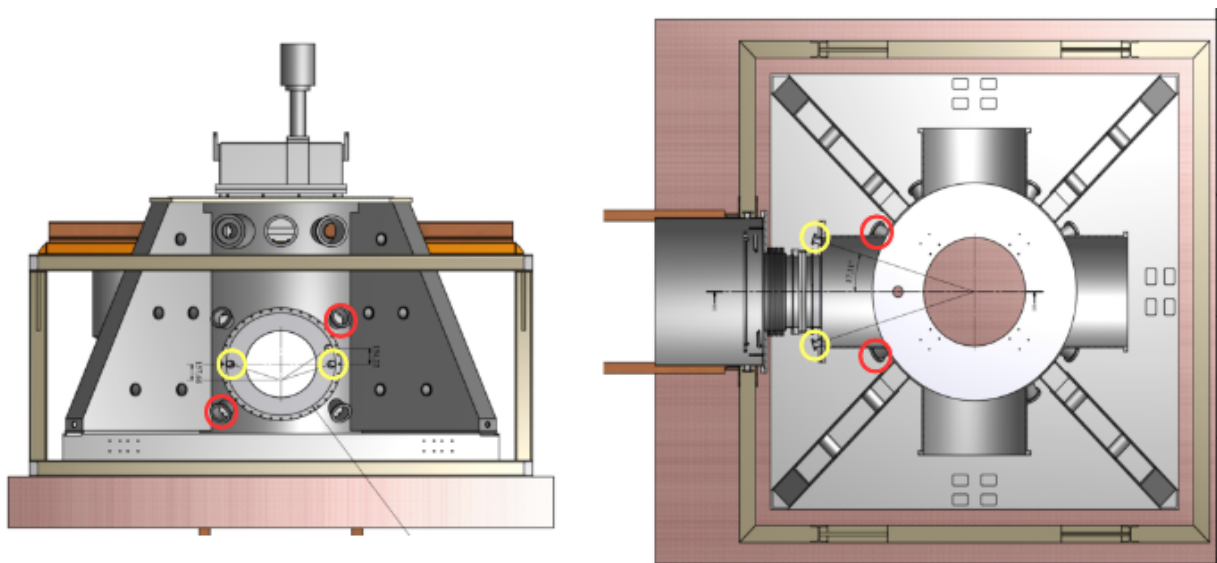


Figure 2: Vacuum tank around end mirrors. Left: side view, from the Fabry-Perot cavity. Right: top view, Fabry-Perot cavity is on the left. Windows for options 1 and 2 are highlighted by circles red and yellow respectively.

the figure 2, it would be convenient to install the PCal injection bench on the left window (with no other window around for an easier access and alignment), and the bench in reflection on the right window (below the other window).

If the access for the "regeneration" procedure could be limited to one side of the tube, it is worth not having it on the side of the PCal injection bench: this will limit the risk to modify the PCal alignment doing the vacuum work. Hence, the most convenient access for the "regeneration" procedure would be on the right side of the tube as shown in figure 2.

## 5.2 Positions of the end mirrors, windows and benches for the PCal (VAC, SAT, PAY, INF)

The position of the end mirror shall be known within of the order of 2 mm in height, laterally and longitudinally.

The relative positions of the two PCal windows wrt the end mirror should be setup within few mm in height, laterally and longitudinally. One important constraints is the symmetry positions of the two windows around the symmetry axis of the mirror.

The absolute position and orientation of the two windows with respect to the center of the tower must be known, after installation, with a precision of a few mm. They must be measured after the installation of the flange.

The relative positions of the two benches must also be known with respect to each other, and with respect to the center of the tower.

Such positions are important for (1) the PCal setup to be possibly installed at the selected location and (2) for a precise estimation of the angle of incidence  $i$  of the PCal beam on the end mirror.

## 5.3 Viewports for the PCal (VAC)

The viewports around the cryotrap are expected to be oriented towards  $\sim 158$  mm below the mirror center. This will properly prevent that a beam reflected on the viewport goes back to the end mirror. The incidence angle of a PCal beam sent horizontally through the viewport is thus  $6^\circ$ .

The viewports have to be coated with anti-reflective coating for the PCal laser wavelength in order to have a transmission coefficient higher than 99.5% for incidence angles around  $6^\circ$ . The wavelength is not yet chosen, but will be between 940 nm and 1140 nm (see section 6.1).

Measurements of the transmission of the viewports with the PCal beam before their installation on the vacuum tank have to be planned. This will help reducing the systematic uncertainties on the reflected power  $P_{ref}$ .

## 5.4 Mass of the end mirror (MIR, PAY)

The mass of the AdV end mirrors will be  $m \sim 42$  kg (twice the mass of the Virgo mirrors).

In order to induce negligible systematic uncertainties on the PCal calibration, the mass  $m$  of the end mirrors, including all the bonded objects, shall be known with a precision of 0.1% (as for Virgo).

## 5.5 Payloads and baffles (PAY, SLC)

Clearance of the payloads and baffles around the PCal beam must be kept, for both 1-beam and 2-beam PCal options.

In the 1-beam configuration, the PCal beam sent through the first window needs to reach the center of the end mirror HR surface and the reflected beam needs to go out the second window. The path around the beam must be cleared from any components of the payload and of the baffles.

In the case of 2-beam configuration, the two PCal beams sent through the first window need to reach the end mirror HR surface symmetrically around its center, with path cleared from any components of the payload and of the baffles. Attention must be paid such that the 2 beams do not hit the electromagnetic actuators. The two reflected beams cannot be recovered outside the vacuum tank. As a consequence, they must be stopped by baffles.

Note that the choice of the windows with the lowest angle of incidence of the PCal beam on the mirror (option 2) decreases the clearance constraints on the payload.

## 5.6 Position of the main ITF beam on the end mirror (ISC)

The position of the main ITF beam on the end mirrors shall have a vertical and lateral tolerance of  $\pm 2$  mm with respect to the center of the mirror to minimize tilt coupling effect in the calibration (see section 6.5 for details).

# 6 Some constraints on the PCal design

## 6.1 Laser wavelength and polarization

The reflection coefficient of the beam on the end mirror, with incidence angle  $i \sim 17^\circ$ , must be as close as possible to 100%, at least 99.5%. With such a high value, it is not needed to measure the beam transmitted through the end mirror (which will not be possible since no viewport allows to measure the beam) and therefore it reduces the power calibration errors. It would also be important that the reflectivity curve is flat around the laser wavelength and incidence angle, such that the uncertainties are low.

Typical reflectivity curve [19] of the HR coating of the AdV end mirrors are shown in figure 3(a). The HR coating is optimized to be flat and close to 100% around 1064 nm. From the curve, the laser wavelength should be between 940 nm and 1190 nm.

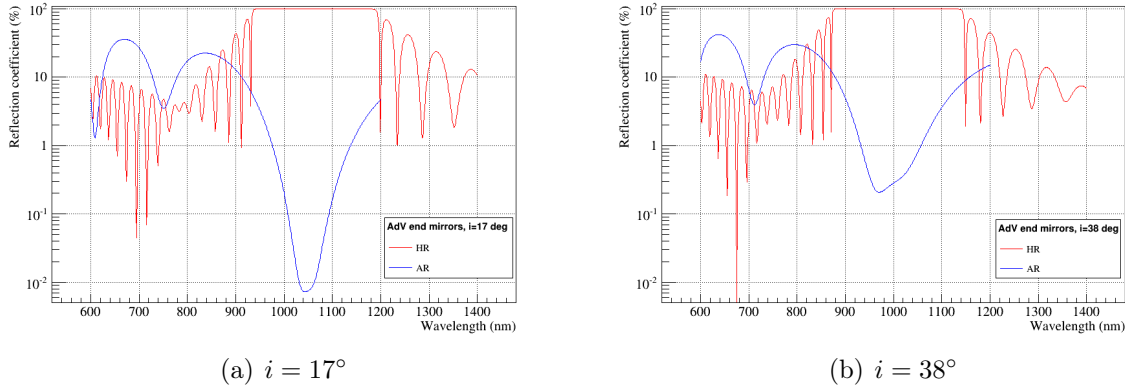


Figure 3: Expected reflectivity curve of the AdV end mirrors as function of wavelength, for an incidence angle  $i$  ( $17^\circ$  or  $38^\circ$ ). Both the HR (red curve) and AR (blue curve) coatings are shown.

The same curve is shown in figure 3(b) for  $i = 38^\circ$ , in the case the viewports of option 1 have to be used. In this case, the condition  $R > 99.5\%$  is valid if the wavelength is between 880 nm and 1140 nm.

As a consequence, in order to be compatible with both viewport solutions, the laser wavelength should be chosen **between 940 nm and 1140 nm**, excluding 1064 nm not to interfere with the main beam.

Note that the exact reflectivity curve might change since studies are on-going to modify the mirror coating to deal with the auxiliary laser beam for the lock acquisition. But in any case, the closer the wavelength is to 1064 nm, the higher its reflection coefficient will be.

These reflectivity curves are given for a s-polarized beam. For a p-polarized beam, the transmission coefficient of the mirror is twice as large, and the flat band has a reduced width. Polarization of the PCal beam will be needed in order to better control its reflection coefficient.

## 6.2 Minimum laser power

### 6.2.1 Permanent lines

Permanent lines sent via the PCal are useful to monitor the stability of the calibration, of the h-reconstruction and of the PCal setup itself. Lines close to the permanent lines sent via the electro-magnetic actuators are planned. Additionally, a line around  $\sim 1$  kHz could be useful to monitor the timing of the reconstructed  $h(t)$  channel.

The table 1 summarizes the expected SNR of the lines measured for a given FFT length. The needed displacement induced by the PCal is then estimated from the noise level expected in AdV sensitivity for two nominal configurations. The curves are reported in appendix B. The

amplitude of the power modulation is also given, both assuming the mirror is a rigid body (i.e. two off-centered PCal beams are used) and taking into account the mirror elastic deformation if a single PCal beam hits the center of the mirror (following the preliminary model described in section 4).

A modulation the PCal laser power with an amplitude close to, but lower than, 100 mW is required to generate permanent lines.

Table 1: Summary of PCal calibration lines for two configurations of AdV: (i) Power recycled, 25 W and (ii) Dual recycled, 125 W, detuned SR. The amplitude of the power modulation of the laser is given assuming the mirror is rigid and taking into account the mirror deformation with a PCal hitting the center of the mirror. The given SNR is given for FFT length of 10 s.

Config	Frequency (Hz)	Noise		SNR	Displacement (m)	Power (mW)	
		( $h/\sqrt{\text{Hz}}$ )	( $\text{m}/\sqrt{\text{Hz}}$ )			rigid	w/ notch
(i)	$\sim 50$	$8.0 \times 10^{-24}$	$2.4 \times 10^{-20}$	100	$7.6 \times 10^{-19}$	0.4	0.4
	$\sim 300$	$1.1 \times 10^{-23}$	$3.3 \times 10^{-20}$	100	$1.0 \times 10^{-18}$	23	23.5
	$\sim 1000$	$3.6 \times 10^{-23}$	$1.1 \times 10^{-19}$	4	$1.4 \times 10^{-19}$	36	44
(ii)	$\sim 50$	$6.8 \times 10^{-24}$	$2.0 \times 10^{-20}$	100	$6.3 \times 10^{-19}$	0.4	0.4
	$\sim 300$	$3.4 \times 10^{-24}$	$1.0 \times 10^{-20}$	100	$3.2 \times 10^{-19}$	7.5	7.7
	$\sim 1000$	$2.6 \times 10^{-23}$	$7.8 \times 10^{-20}$	4	$1.0 \times 10^{-19}$	26	32

### 6.2.2 Calibration up to 1 kHz

A reasonable goal for the PCal calibration data is to measure  $\sim 100$  points logarithmically spaced between 10 Hz and 1 kHz in 1 hour, with precision of 1% on the ratio dark fringe signal over PCal line. Such data are needed to cross-check the actuator calibration and the  $h(t)$  reconstruction.

This is possible assuming successive lines with PCal laser amplitudes of  $\sim \pm 100$  mW and with the nominal AdV sensitivity curves.

### 6.2.3 Hardware injections

Exciting the mirrors with the PCal to apply the hardware injection is appealing, in particular in the case of the blind injection challenge since the PCal actuator is not used in the control loop of the detector. However, this induces the need to inject typical source signals with the proper amplitude and over the full band-width of the signals.

In order to estimate the power needed to be injected by the PCal laser to perform such hardware injections, the  $h(t)$  time series of different GW signals have been simulated:

- a coalescence of a binary neutron star (BNS), with two neutron stars of  $1.4 M_{\odot}$  each, located at 20 Mpc, on top of Virgo interferometer, where the antenna response is maximum.

- a coalescence of a binary black hole (BBH), with two black holes of  $10 M_{\odot}$  each, located at 20 Mpc, on top of Virgo.
- a burst signal simulated as a sine-gaus signal with a frequency of 1 kHz and amplitude  $10^{-20}$ .

The CBC worst case scenario (i.e. higher laser power needed) is the BNS signal since it is the CBC signal going up to the higher frequencies, of the order of 1.5 kHz. The maximum frequency of the signal is important since the mechanical response decreases with energy, hence higher power is needed to apply a given signal  $h(t)$  at higher frequency. The CBC signals have been generated using lalsuite package, version v6r25. An option of the simulation is the presence of tapering at the end of the simulated strain. Results are shown with and without tapering. See appendix C to have more details on the simulation parameters and more figures (signal FFTs or useful zoom on the time-series).

The inverse of the PCal response function described in section 4 is then applied to the simulated  $h(t)$  time series in order to estimate the time series of the laser power to be applied on the mirror to simulate such a signal in the interferometer. The simple pendulum response (rigid mirror) and the model which takes into account the mirror elastic deformations have both been used in this study.

The package HInjection, version v0r16, has been used to convert the  $h(t)$  time series into the laser power time series: the inverse mechanical response has been applied to the  $h(t)$  time series. The configuration file of the HInjection process is reported in appendix C.3. HInjection applies the filter in the frequency domain – doing FFT of the strain signal over 2 s and applying the filter transfer function (with a sharp cut at  $\sim 2$  kHz) – and computes the inverse FFT to get back the PCal power time series.

In parallel, the strain time series has been filtered in the time-domain defining the filter as an IIR filter with Frv tools. In this case, a 4th order low-pass filter has been added at 5 kHz. It is necessary in the case of a rigid mirror since the pendulum inverse transfer function diverges in  $f^2$ .

The plots shown here are the ones from the second method, but the results of both methods are very similar, within  $\sim 10\%$ , which comes mainly from the way the high frequency part is dealt with (sharp cut-off or low-pass).

The time series of the simulated  $h(t)$  and of the needed laser power for different mechanical responses (rigid mirror and elastic mirror) are shown in figure 4, with tapering (red) and without (black). Without tapering, the presence of a step at the end of the inspiral signal generates ring-down effects that are much higher than the power one really wants to inject to simulate the CBC. It shows that tapering is necessary when simulating an inspiral-only signal. The power shown in red are thus the ones really needed to apply hardware injections with the PCal: in the case of the BBH, the maximum power is 70 mW (see also figure 12), but, in the worst-case BNS scenario, the maximum power reaches 1 W.

In the case of burst-like sine-gaussian signals, the times series are shown in figure 5. The

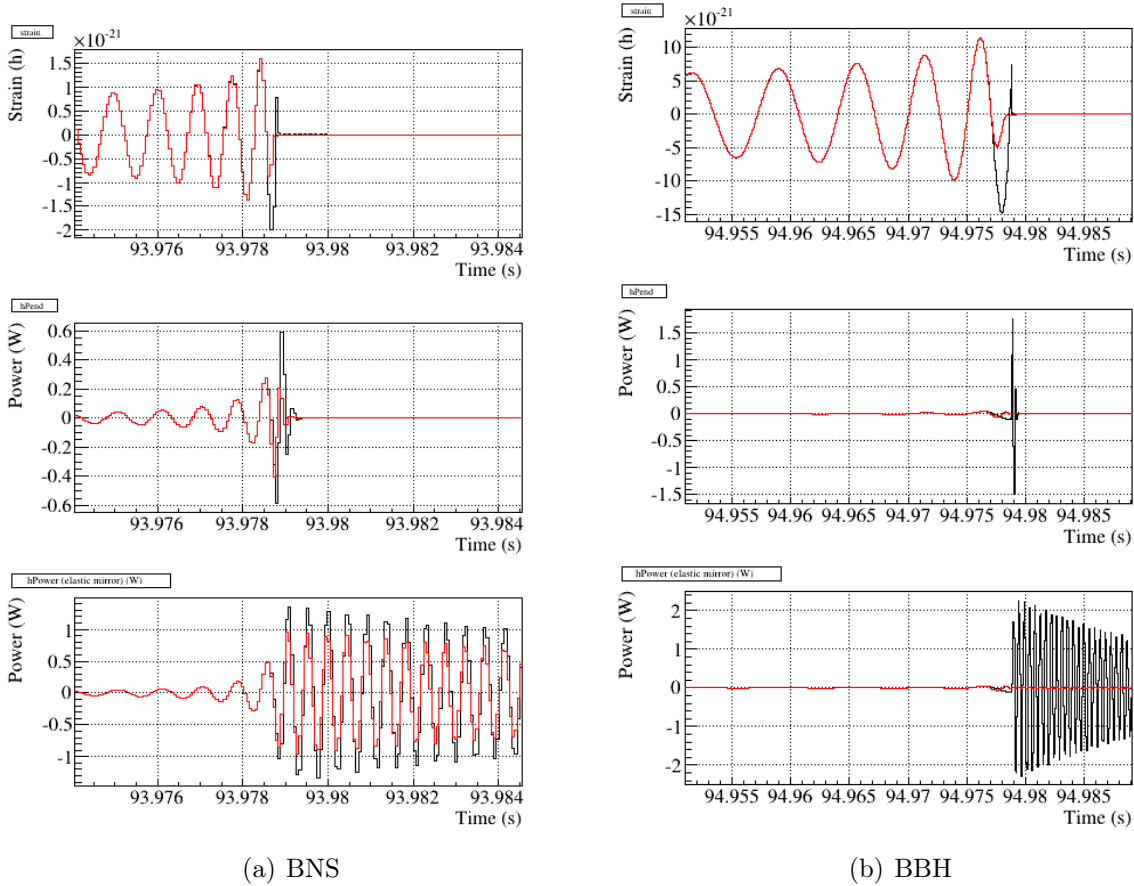
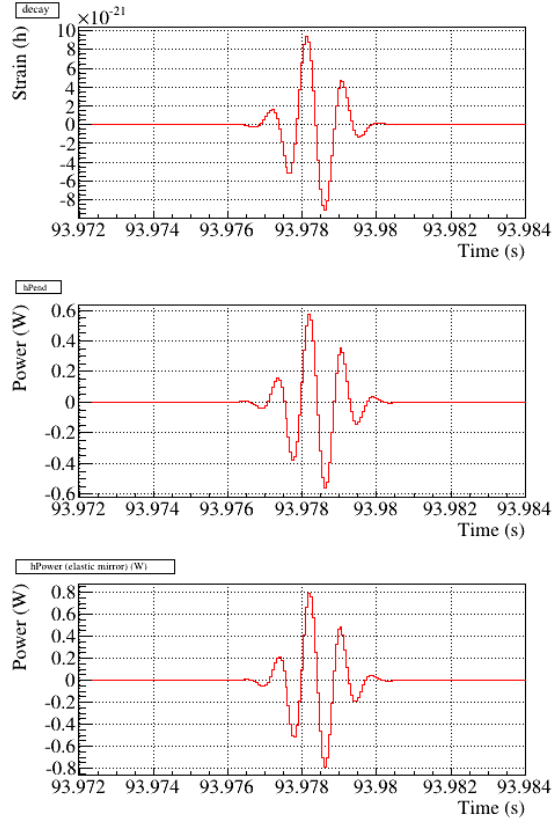


Figure 4: Example of the PCal laser power needed to inject a CBC signal (BNS or BBH) for a source located above the Virgo interferometer, at a distance of 20 Mpc. Only the last cycles of the CBC signals are shown. Two different simulations were done: with (red) or without (black) tapering of the end of the times series; top: time series of the simulated  $h(t)$  signals of the CBC. middle: time series of the derived power to be generated by the PCal in the case of a rigid mirror. bottom: time series of the derived power to be generated by the PCal in the case of an elastic mirror. A y-zoom of the BBH last cycles can be found in figure 12.

maximum power reaches almost 1 W also. Note that the needed laser power increases if the burst has a higher frequency. Hence the injection of bursts with the PCal might be limited to low amplitude signals. It will need to be better studied later.

To conclude, in order to perform hardware injections of CBC or burst signals with reasonable SNR, the laser must be modulated up to  $\sim \pm 1$  W, i.e. it is needed to choose a laser with a maximum power of at least  $\sim 2$  W. Even BNS signals could be injected, but this will need to be confirmed with the installed PCal setup, after having measured the real mechanical response of the PCal, which will depends on the exact frequency of the mirror internal mode and its



(a) Burst at 1 kHz

Figure 5: Example of the PCal laser power needed to inject a burst signal (sine-gaus signal at 1 kHz, with amplitude  $10^{-20}$ ). top: time series of the simulated  $h(t)$  signals of the burst. middle: time series of the derived power to be generated by the PCal in the case of a rigid mirror. bottom: time series of the derived power to be generated by the PCal in the case of an elastic mirror.

exact level in the PCal response. Also, the range of the pairs frequency-amplitude of the bursts signals that can be injected by the PCal will be precisely defined when the mechanical response will be known.

#### 6.2.4 Conclusion

Amplitudes of the order of  $\pm 100$  mV around the average laser power are enough to inject the permanent PCal calibration lines and perform the cross-check of the actuator calibration and of  $h(t)$  reconstruction. Higher amplitudes of  $\pm 1$  W are needed to be able to perform typical hardware injections.

In order to apply these four types of measurements and keep the laser power modulation not too close to 0 W at its minimum, **a laser with a maximum power of at least  $\sim 3$  W is needed.**



### 6.3 Power noise

The amplitude spectral displacement noise from the PCal should not exceed 10% of the design sensitivity of AdV. It puts constraints on the noise of the laser power. The power noise requirements have been derived for both the cases of a rigid mirror and a mirror with elastic deformations induced by the single-beam PCal. They are shown in the figure 6. Note that, since the power of the laser is of the order of a watt, the level of the relative intensity noise (RIN) has values of the same order, but given in  $1/\sqrt{Hz}$ .

Such a noise level is reachable, possibly with the addition of a control loop of the laser power.

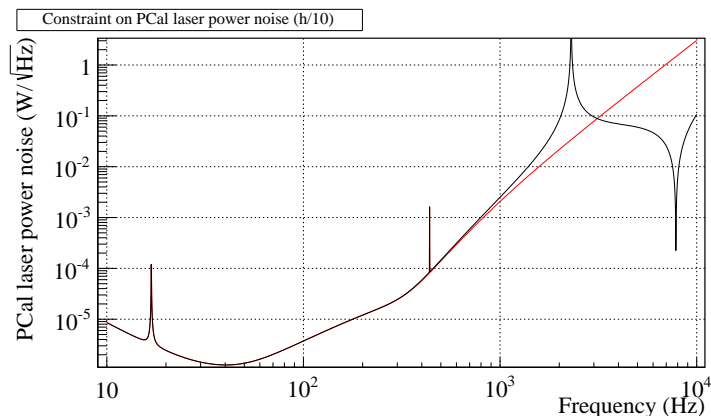


Figure 6: Power noise requirement for the AdV PCal laser. Black: case of a rigid mirror. Red: case of an elastic mirror, with the PCal beam hitting the center.

Constraints on the presence of harmonics of the permanent lines can also be put. The assumed requirement is that any harmonic line should have a SNR lower than 0.1 in the amplitude spectral density of the AdVirgo gravitational wave signal  $h(t)$  calculated with FFT of duration 10 s.

The constraints have been estimated assuming a calibration line is generated at 50 Hz. They must be close to the stongest constraints since the harmonics of few hundreds of hertz fall in the region with the better sensitivity of AdV. Taking the number of table 1, it is assumed that a sine with amplitude 0.4 W is generated as the main calibration line at 50 Hz. The constraints on the first harmonics of this calibration line are summarized in the table 2. Non-linearities in the calibration line generation can generate harmonics but must be kept below -50 dB. The non-linear noise of the DAC1955 channel that will be used to control the laser power generate harmonics whose levels are much lower, below -100 dB [16]. Hence the constraints given in the table apply to the tool used to modulate the PCal laser power, either the PCal laser control itself, or an AOM if this option is chosen.

Table 2: Constraints on the harmonics of the permanent calibration lines of AdV. The case of calibration line at 50 Hz has been chosen as a reference. The level of the sensitivity curve used in this estimation is given. Then, the maximum amplitude of the induced mirror displacement and of the laser power harmonic line are given at the first harmonic frequencies. The first line recall the needed parameters to generate a permanent line with SRN 100 in 10 s at 50 Hz. The last column gives the constraints on the attenuation of the harmonic lines.

Frequency (Hz)	Noise ( $h/\sqrt{\text{Hz}}$ )	Displacement (m)	Power ( $\mu\text{W}$ )	Attenuation (dB)
$\sim 50$ (SNR 100)	$6.8 \times 10^{-24}$	$6.3 \times 10^{-19}$	$0.4 \times 10^3$	–
100	$4.8 \times 10^{-24}$	$4.6 \times 10^{-22}$	1.2	-50
150	$4.0 \times 10^{-24}$	$3.8 \times 10^{-22}$	2.2	-45
200	$3.9 \times 10^{-24}$	$3.7 \times 10^{-22}$	3.8	-40
250	$3.5 \times 10^{-24}$	$3.3 \times 10^{-22}$	5.4	-37
300	$3.3 \times 10^{-24}$	$3.1 \times 10^{-22}$	7.3	-35

## 6.4 Laser beam profile

One of the main source of systematic errors when calibrating the power of the PCal beam in Virgo was due to its large size at the reflection and transmission ports. Some optical components were needed in order to focus the beam on the powermeter sensor ( $\sim 1 \text{ cm}^2$  active area).

In order to measure at least 99.9% of the PCal beam power directly on the sensor, the beam radius must be lower than  $1/3.3\text{th}$  of the sensor radius. Assuming similar sensors as used in Virgo, with radius  $\sim 5 \text{ mm}$ , the beam radius must be below  $1.7 \text{ mm}$ .

Assuming a TEM00 beam, a waist of  $\sim 670 \mu\text{m}$  located close to the end mirror is a possible solution. A telescope on the injection bench will be designed to adapt the laser beam.

## 6.5 Alignment of main and PCal beams on the mirror

When the PCal force is not directed through the center of mass of the mirror, the induced torque causes an angular deflection of the mirror. The resonance frequencies for pitch and yaw rotations of the suspended mirror are  $\sim 0.5 \text{ Hz}$ . The mirror is freely rotating for modulation frequencies much greater than these resonance frequencies. If the ITF beam is not centered, then the interferometer senses an apparent mirror motion due to its rotation.

Following [8], let's call  $\vec{a}$  and  $\vec{b}$  the displacement vectors of the PCal and main beams from the center of the mirror, and  $I$  its moment of inertia ( $I = ml^2/12 + mr^2/4$  where  $l = 0.200 \text{ m}$  and  $r = 0.175 \text{ m}$  the mirror thickness and radius). The effective mirror motion seen by the ITF is:

$$\Delta x_{\text{rigid,rot}}(t) = -\frac{1}{m} \frac{2 \cos(i)}{c} \frac{\Delta P_{\text{ref}}(t)}{(2\pi f)^2} \left( 1 + \frac{\vec{a} \vec{b} m}{I} \right) \quad (2)$$

The relative error induced on the effective mirror motion in case of beam misalignment is shown

in figure 7 for PCal beam misalignment up to 5 cm and for different main beam misalignment <sup>1</sup>.

This effect can be neglected ( $< 0.4\%$ ) if the main beam is centered within 2 mm on the center of the mirror and the PCal beam is centered within 2 cm.

It is worth noting that the mirror rotation induced by a misaligned PCal beam is negligible for what concerns the Adv alignment and sensitivity. The induced rotation can be estimated as:

$$\Omega(\omega) = -\frac{2|\vec{a}|P_{ref} \cos(i)}{I_C \omega^2} \quad (3)$$

For an offset  $a$  of 1 cm and an injected line of amplitude 100 mW at 10 Hz, the induced rotation is  $\sim 3.5 \times 10^{-15}$  rad, much lower than the  $\sim 100$  nrad requirements on the end mirror angular control [11].

**1-beam configuration** – In the case of a single PCal beam hitting the center of the mirror, the beam position on the mirror can be estimated geometrically from the positions of the beam on the viewports. Uncertainties are of the order of 1 cm as shown in Virgo+ [5].

**2-beam configuration** – In the case of a 2-beam configuration, the reflected beams are lost and no geometrical reconstruction of the position of the beams on the mirrors can be done. In order not to rotate the mirror, the line of the two beams must contain the center of the mirror

<sup>1</sup> During Virgo, the main beam offset was precise [20] within at most 5 mm. It could have been checked and improved down to  $\sim 2$  mm. The PCal beam was centered [4, 5] within 2 cm.

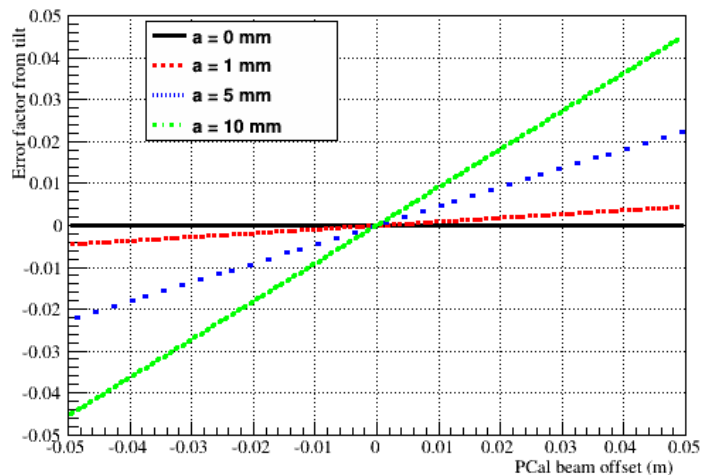


Figure 7: Relative error induced on the effective mirror motion in case of beam misalignment (offsets  $\vec{a}$  and  $\vec{b}$  are assumed to be parallel).

surface, and the forces balanced. The two beams will not have the same angle of incidence on the mirror,  $\sim 15^\circ$  and  $\sim 22^\circ$ , which must be compensated by slightly different powers of the two beams, by  $\sim 4\%$ . Moreover, the beams must be carefully positioned with respect to the positions of the electromagnetic actuators.

**Monitoring of the beam alignment** – It will be useful to monitor the long term beam alignment using a quadrant photodiode. In particular, the PCal benches will be located in areas without a lot of space around but where VAC people will need to work from time to time to maintain the cryotrap. Hence the monitoring will allow to check that the PCal setup was not misaligned during such operations, and to take care of re-aligning it if necessary. In the case of 1-beam PCal, the quadrant will be placed in reflection of the end mirror. In the case of a 2-beam PCal, the quadrant will be placed on the injection bench, providing less information: in case the whole bench position is modified, it will not be seen by the quadrant.

An additional way to monitor the PCal alignment could be to use the IR camera monitoring the end mirror: if some light from the PCal beam is diffused on the HR coating of the mirror and is visible on the camera, it can be used first to align the PCal beam during the installation phase, and then to monitor the beam position, but only from time to time (since it will be needed to dump the main ITF beam to observe potential PCal beam diffusion).

## 6.6 Power calibration and choice of the powermeter

The calibration of the PCal consists in calibrating the monitoring photodiode signal as a function of the power of the beam reflected onto the end mirror as stated in equation 1. A powermeter has to be inserted onto the beam paths on the injection bench and on the reflection bench (in the case of single beam configuration) right before and after the viewport respectively. Some free space must be kept in the optical layout of the PCal benches to insert the powermeter head. Assuming similar powermeter sensors as in Virgo, without the motors that were used for scanning the beam, free space of  $\sim 10\text{ cm} \times 10\text{ cm}$  must be enough. With the motors, space perpendicular to the beam axis must be increased to at least 15 cm.

Since the force applied on the mirror depends on the absolute power, the powermeter and its sensor head must be calibrated by NIST. Regular re-calibration must be planned to limit any time variation of the powermeter response.

In order to limit the systematic errors, 99.9% of the beam power must enter the powermeter sensor head. Taking into account some possible misalignment of  $\sim 2\text{ mm}$  of the beam on the sensor, the radius  $r$  of the sensor must be  $r \geq 3.3w + 2\text{ mm}$  where  $w$  is the beam radius at the measurement position.

The homogeneity of the powermeter sensor must be carefully measured in order to estimate systematic errors coming from the powermeter.

A way to limit systematic errors coming from the sensor inhomogeneities and from beam inclination on the sensor is to use an integrating sphere that spreads the incoming light onto

all the sensor surface<sup>2</sup>. Of course, in this case, the NIST calibration has to be done for the system {integrating sphere + sensor}. A priori, a sphere with 0.5 inch (1.27 cm) input port diameter must be enough. The corresponding sphere have a diameter of 2 inches (5.08 cm), onto which the sensor head and some connectors are plugged. The space needed to insert such an integrating sphere must be at least  $\sim 10 \text{ cm} \times 10 \text{ cm}$ .

A cross-check of the LIGO et Virgo cross-calibration can be done by exchanging the powermeters used in both experiments to perform the calibration of the other sites. To be completely compliant, the laser wavelengths of the LIGO and Virgo PCal's should be the same, which might not be the case. A powermeter with flat response in a band including all the PCal laser wavelengths could be a good solution to be investigated. The wavelength of the LIGO PCal laser is planned to be 1064.?? nm. So the closest the Virgo PCal laser is to this wavelength, the easiest will be such cross-calibration measurements.

## 6.7 Timing synchronization and timing calibration

The PCal must be synchronized on the GPS via the timing distribution system. A setup for timing calibration must be setup.

The setup used for timing calibration in Virgo can be used [3]: some generated wide-band signal is sent to a time-calibrated ADC channel and to a red LED in front of the monitoring PCal photodiode. The delay between the two signals is used to calibrate the PCal timing. Some redundancy can be obtained if the signal is a clock or the IRIG-B signal.

## 7 Possible ideas

Here is a list of some pending questions to be checked and of some possible ideas to improve some properties of the PCal setup. They are not discussed in this note:

- check that injecting a signal onto only one of the end mirror is really equivalent to injecting half of the signal onto the two end mirrors. The question must be yes in case the two arms are symmetric, but might be studied in more details in the case of finesse asymmetry in particular.
- a way to increase the PCal actuation with a given laser power is to reflect back on the PCal reflection bench the beam reflected by the end mirror towards the end mirror again and injection bench: having the beam hitting the end mirror twice would increase the PCal actuation by almost a factor 2.

---

<sup>2</sup> Integrating spheres 819C-SL-2-CAL2 or 819C-IG-2-CAL from Newport could be convenient, with maximum measurable power of  $\sim 1.5 \text{ W}$  to  $\sim 2 \text{ W}$ , and 2.5% to 2% calibration uncertainties. Their cost is of the order of 2800 €. These integrating spheres provide a small pick-off on an optical fiber that can be used to measure the laser wavelength and hence precisely select the powermeter working point and calibration.

Another idea was to inject PCal lines when the interferometer is configured in free swinging Michelson (configuration used to calibrate the mirror actuators with the standard method [17]). However, the sensitivity of such measurements is such that, in order to see the injected PCal lines, laser power amplitudes of  $\sim 10$  W to  $\sim 1$  kW would be needed; which is not possible.

## 8 Summary

In this note, a conceptual design of the Advanced Virgo photon calibration setup has been described. The pros and cons of the PCal used during Virgo have been important inputs for this new design. To summarize the main features of the new setup, two PCal setups will be installed, one around each end mirror ; a single PCal laser beam hitting the center of the mirror is foreseen, but, if possible, the option to go for a two-beam PCal setup will be kept when designing the optical benches ; the laser power must be of the order of 3 W in order to perform hardware injections with the PCal setup, with constraints on its power noise in order to be kept below the AdV sensitivity curve ; the PCal upgrade will take into account the difficulties encountered during Virgo to perform an accurate power calibration of the beam.

With the foreseen setup, the four main goals of the PCal will be reachable:

- direct verification of the sign of the reconstructed  $h(t)$  channel,
- cross-check of the standard electro-magnetic actuator calibration and  $h(t)$  reconstruction,
- permanent monitoring to assess the stability of the electro-magnetic actuators and of the  $h(t)$  reconstruction,
- application of hardware or blind injections of short GW-like signals in the ITF.

## References

- [1] B. Mours and L. Rolland, Virgo note [VIR-0018A-07](#) (2007) *Determining the sign of h-rec with the photon calibrator*
- [2] B. Mours and L. Rolland, Virgo note [VIR-0534A-08](#) (2008) *Use of the photon calibrators for the VSR1 calibration*
- [3] T. Accadia, L. Rolland and B. Mours, Virgo note [VIR-0404A-10](#) (2010) *Power and timing calibration of the Photon Calibrator for VSR2*
- [4] T. Accadia, [PhD thesis report](#) (2012) *Vérification de la reconstruction du signal d'onde gravitationnelle de Virgo à l'aide d'un dispositif d'étalonnage utilisant la pression de radiation laser*
- [5] T. Accadia et al. (Virgo collaboration), CQG **31** 165013 (2014) *Reconstruction of the gravitational wave signal  $h(t)$  during the Virgo science runs and independent validation with a photon calibrator*
- [6] K. Mossavi et al, Phy. Lett. A 353 1–3 (2006) *A photon pressure calibrator for the GEO 600 gravitational wave detector*
- [7] S. Hild et al., Class. Quantum Grav. 245681-8 (2007) *Photon-pressure-induced test mass deformation in gravitational-wave detectors*
- [8] E.Goetz et al., Class. Quant. Grav. Vol. 26, pp. 245011-23 (2009) *Precise calibration of LIGO test mass actuators using photon radiation pressure*
- [9] S. Vitale, LIGO talk [G1300788-v2](#) (2013) *Calibration requirements for CBC in the Advanced Detector Era*
- [10] E. Thrane for the "Stochastic group", LIGO note [T1200562-v1](#) (2012) *Calibration requirements for stochastic searches in the advanced detector era*
- [11] The Virgo collaboration, *Advanced Virgo Technical Design Report* (2012) [VIR-0128A-12](#).
- [12] L. Lindblom, Physical Review D 80 042005 (2009) *Optimal calibration accuracy for gravitational-wave detectors*
- [13] K. Kawabe, L. Rolland and X. Siemens, [talk LIGO-G1000274](#) (2010) *Calibration in the Advanced Detector Era*
- [14] J. Berliner and R. Savage, [note LIGO-T1100044](#) (2011) *Photon Calibrator Design Requirements*
- [15] P. Daveloza, [talk LIGO-G1200900](#) (2012) *aLIGO Photon Calibrators Calibration*

- [16] N. Letendre et al., Virgo note [VIR-0170A-14](#) (2014) *First tests of the DAC1955 mezzanine (version 1)*
- [17] T. Accadia et al. (Virgo collaboration), CQG [20 025005](#) (2011) *Calibration and sensitivity of the Virgo detector during its second science run*
- [18] Private discussions with A. Pasqualetti
- [19] Private discussions with L. Pinard
- [20] Private discussions with P. Ruggi



## A Optocad simulations to select the windows for the PCal

As described in section 5.1, two possible window configurations were envisaged. The option 2 (use of new AdV windows around the cryotrap) have some advantages, except for the aperture of the viewports.

In this appendix, the Optocad<sup>3</sup> simulations that were done to check that the PCal setup can be installed using option 2 are described. The main constraints are (i) that the reflected beam goes out through the reflection viewport in the case of the single-beam configuration, and (ii) that it is possible to send two beams symmetrically around the mirror center in the case of the two-beam configuration.

In the simulation, the end mirror is located at the center of the tower, and with a thickness of 200 mm. The wall of the vacuum enclosure is set 1.5 m away from the center of the mirror.

The horizontal section of the flange is drawn. It is assumed that the vacuum side of the flange has an aperture of 63 mm in this section. The on-axis length of the flange is 80 mm. The horizontal angle of the flange is 17.12°, towards the center of the tower. Since the flange axis is oriented 6° below the horizontal plane (below the mirror), the cross-section of the flange cylinder in the horizontal plane has been drawn.

The PCal beam is supposed to be horizontal, at the level of the center of the mirror. It is simulated with a waist of 700  $\mu\text{m}$  located close to the end mirror. A telescope will be needed on the injection bench to reach this beam size.

The benches are drawn as blue rectangles. Their size is supposed to be 25 cm  $\times$  50 cm and 25 cm  $\times$  25 cm for the injection and reflection benches respectively. A yellowish square of 10 cm  $\times$  10 cm has been drawn on the benches: it represents the typical zone needed to be free to insert a powermeter for PCal calibration.

### A.1 Single beam PCal configuration

A conceptual layout is shown in figure 8 in the case of a single beam hitting the center of the end mirror.

A pick-off is sent to a photodiode on the injection bench in order to monitor the injected power and to estimate the force induced on the end mirror. The reflected beam is sensed on a quadrant photodiode on the reflection bench in order to monitor the setup alignment.

The simulation has shown that the reflected beam goes out through the reflection window, which is necessary for the PCal power calibration and for the PCal beam alignment (using viewport positions).

In this layout, the PCal beam enters with an offset of  $\sim 15$  mm from the center of the input viewport, and goes out with an offset of  $\sim 15$  cm at the output. This confirms that tolerances of up to 1 cm on the position of the windows are satisfactory. Moreover, the large input offset is due to the fact that the mirror b1\_M1 has a position that can be used for the two-beam

---

<sup>3</sup>Optocad version: 093j.

configuration also. If only the single beam configuration is setup, the beams can be better centered on the viewports.

With such a "simple" layout, there is some space to insert a telescope between the laser output and the mirror M1, and there is some space to insert a powermeter during the photodiode calibration, both on the injection and on the reflection benches.

## A.2 Two-beam PCal configuration

A conceptual layout is shown in figure 9 in the case of two beams hitting symmetrically around the center of the end mirror. In this simulation, the beams hit the mirror at 100 mm from the center of the HR surface.

A photodiode is used on the injection bench to monitor the beam from the PCal laser before it is split in two. The two split beams are monitored on the injection bench with a photodiode for power calibration and a quadrant to monitor the alignment.

The reflected beams do not go out the end tower and have to be dumped by baffles.

With this layout, the bench is crowded and optimization with mechanical CAO will be needed to check the space between mirror mounts. There is not a lot of space left for the telescope nor for the powermeter in front of the viewport.

Note that the positions of the mirror up to b1\_M1 are the same as for the single-beam configuration. It might be possible to have a setup that allows to switch between single- and two-beam configurations. However, some motorized mounts and flippers would be needed to switch, which is challenging when looking to the low space between mounts.

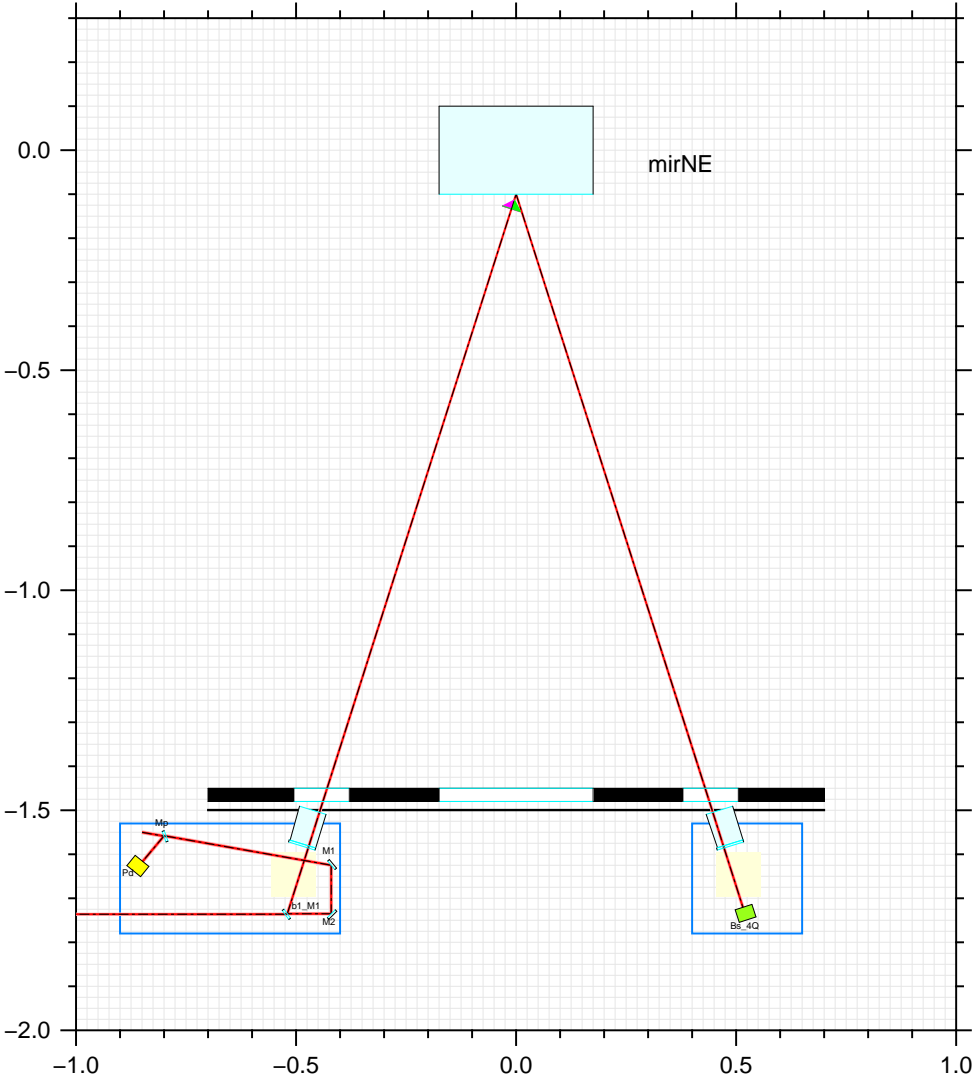


Figure 8: Single beam configuration.

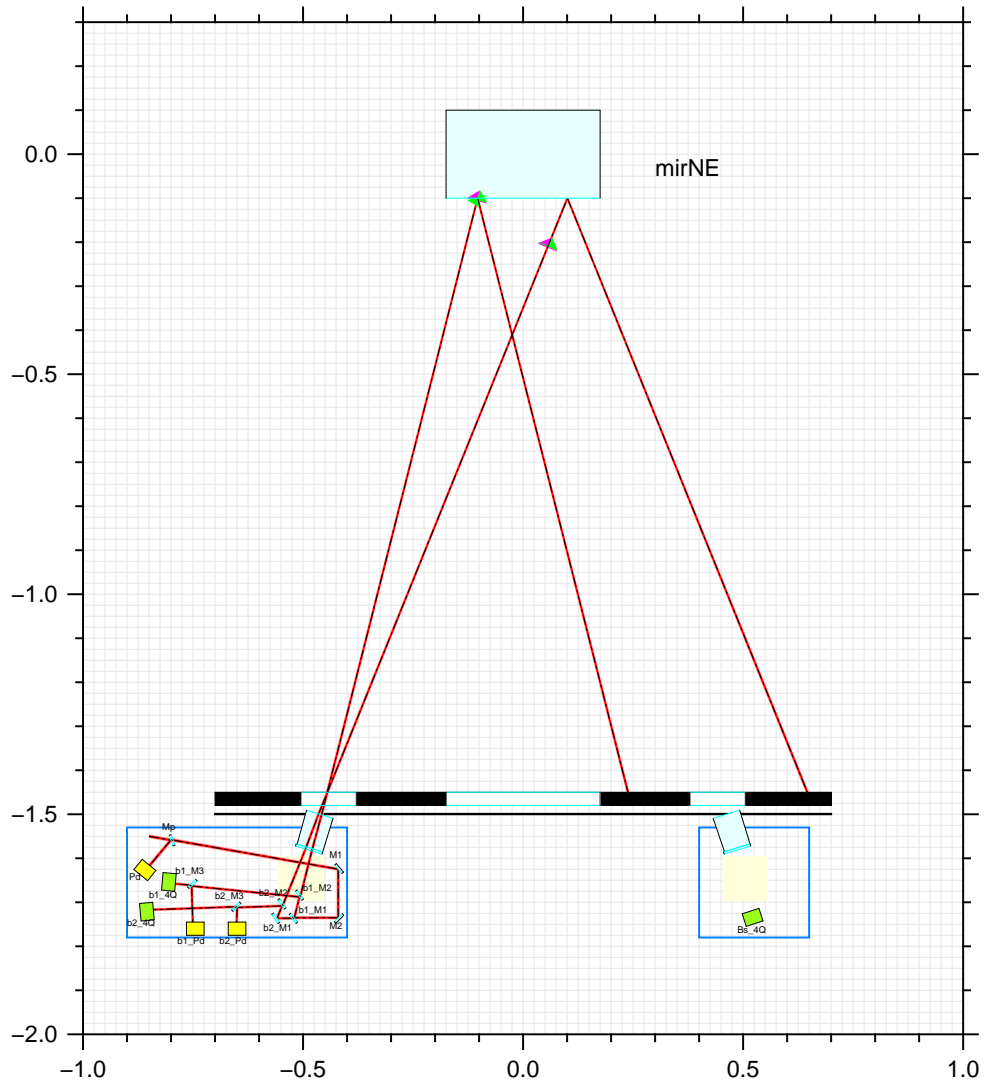


Figure 9: Two-beam configuration.

## B AdV reference sensitivity curves

For reference, the sensitivity curves of AdVirgo in different nominal configurations are reported here. The figure is extracted from the TDR [11].

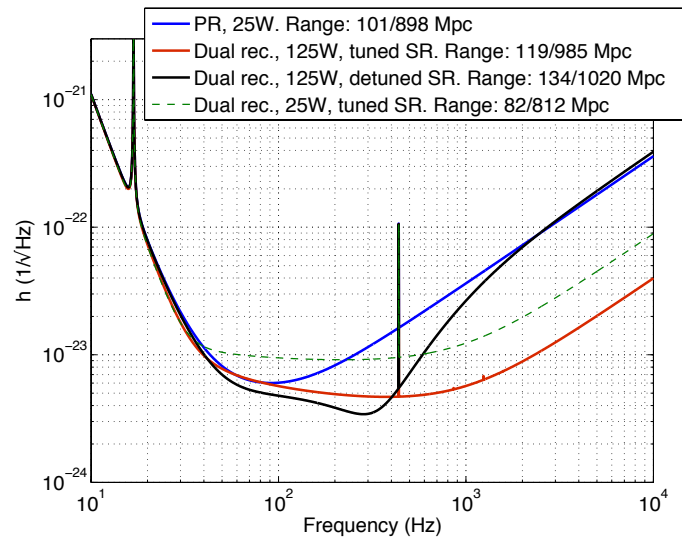


Figure 10: Reference sensitivity curves for a possible evolution of AdV configuration.

## C Details about hardware injections

### C.1 BNS signal simulation: generation script using lalsuite

```
#!/bin/bash

FILE=injection_file.xml

TIME=1127687716
lalapps_inspinj --output ${FILE} --seed 1 --f-lower 35 --gps-start-time ${TIME} --gps-end-time ${TIME}+1 --time-step 2200
                --i-distr fixed --fixed-inc 0.
                --l-distr fixed --longitude 0 --latitude 43.63
                --d-distr volume --min-distance 19999 --max-distance 20001
                --m-distr fixMasses --fixed-mass1 1.4 --fixed-mass2 1.4
                --disable-spin
                --waveform SpinTaylorT4threePointFivePN --taper-injection startend
                --ligo-fake-psd LALAdLIGO --virgo-fake-psd LALAdVirgo

lalapps_coinj --input ${FILE} --output-path . --response-type etmy --frames

echo "Generated waveforms"
MASS1='lwtprint -t sim_inspiral -c mass1 ${FILE}'
MASS2='lwtprint -t sim_inspiral -c mass2 ${FILE}'
DIST='lwtprint -t sim_inspiral -c distance ${FILE}'
RA='lwtprint -t sim_inspiral -c longitude ${FILE}'
DEC='lwtprint -t sim_inspiral -c latitude ${FILE}'
GCEND='lwtprint -t sim_inspiral -c geocent_end_time ${FILE}'
GCENDNS='echo "$(lwtprint -t sim_inspiral -c geocent_end_time_ns ${FILE} ) * 0.000000001" | bc -l'
HEND='lwtprint -t sim_inspiral -c h_end_time ${FILE}'
HENDNS='echo "$(lwtprint -t sim_inspiral -c h_end_time_ns ${FILE} ) * 0.000000001" | bc -l'
LEND='lwtprint -t sim_inspiral -c l_end_time ${FILE}'
LENDNS='echo "$(lwtprint -t sim_inspiral -c l_end_time_ns ${FILE} ) * 0.000000001" | bc -l'
VEND='lwtprint -t sim_inspiral -c v_end_time ${FILE}'
VENDNS='echo "$(lwtprint -t sim_inspiral -c v_end_time_ns ${FILE} ) * 0.000000001" | bc -l'

echo ""
echo "Mass 1 = $MASS1 Msun"
echo "Mass 2 = $MASS2 Msun"
echo "Distance = $DIST Mpc"
echo "Right Ascension = $RA rads"
echo "Declination = $DEC rads"
echo "tC at Geocentre = ${GCEND}.${GCENDNS#.}"
echo "tC at Hanford = ${HEND}.${HENDNS#.}"
echo "tC at Livingston = ${LEND}.${LENDNS#.}"
echo "tC at Virgo = ${VEND}.${VENDNS#.}"
echo "Network SNR = $SNR"
```

### C.2 BNS signal simulation: terminal output

```
>> ./make_injection.sh

Injected signal 0 for H1 into file ./1127687621_CBC_BNS_0_ETMY_H1.txt
SNR in design H1 of injection 0 = 4.995486
Generating frame file for H1-INSP0-HWINJ-STRAIN-1127687621
Injected signal 0 for L1 into file ./1127687621_CBC_BNS_0_ETMY_L1.txt
SNR in design L1 of injection 0 = 4.489284
Generating frame file for L1-INSP0-HWINJ-STRAIN-1127687621
SNR in design V1 of injection 0 = 10.694657
Generating frame file for V1-INSP0-HWINJ-STRAIN-1127687621

Network SNR of 0 = 12.628707
```

## Generated waveforms

```

Mass 1 = 1.39999998 Msun
Mass 2 = 1.39999998 Msun
Distance = 20.0002804 Mpc
Right Ascension = 0 rads
Declination = 0.761487186 rads
tC at Geocentre = 1127687716.0
tC at Hanford = 1127687715.996426862
tC at Livingston = 1127687715.995490171
tC at Virgo = 1127687715.978761879
Network SNR =

```

### C.3 Configuration file of HInjection process

```

CFG_PRIO 3 # Main priorit 0 means no change (nice(0))
CFG_NOFILESAVE
CFG_NOBDBSAVE # No commit into Db
CFG_CMDDOMAIN NONE
CFG_PWD /home/rolland-local/VIRGO/virgoLog/HInjection # Current logfile path <path>/<cmName>
CFG_RFLAG eloff # Report flags: el{on,off}, stdout{on,off}, log{on,off}

FDIN_FILE /home/rolland-local/VIRGO/virgoData/ffl/trend_fake.ffl 1102809600 1800
FDIN_FRAME_DURATION 1
HINJ_SAMPLE_RATE 10000

# Gain of the PCal TF: -TMath::C()*42 * 3000./2./cos(17*TMath::Pi()/180) for m = 42 kg, L0 = 3000 m, i = 17 deg

#HINJ_TF name gain delay_s fmin_Hz fmax_Hz FFTduration_s
HINJ_TF TF_PCal -1.97e+13 0 10. 3000. 2 #used for Adv PCal Conceptual Design note
HINJ_ZERO 0.6 1000. #Pendulum response
HINJ_POLE 2300 100 # approximation of the notch

HINJ_TF TF_Flat 1 0 10. 4000. 2 #used for Adv PCal Conceptual Design note
HINJ_NOISE NOISE_WHITE 0.001 1102809610 1800 NONE
HINJ_NOISE NOISE_FILTERED 0.001 1102809610 1800 TF_PCal

##HINJ_FILE filename input output scaling GPSstart InjDuration TFname
HINJ_FILE V1-INSP0_HWINJ_STRAIN-1127687622_tapered-100.gwf V1:FAKE-STRAIN_INJ Ca_PCal_Power_4R 1. 1102809610 1600 TF_PCal
HINJ_FILE V1-INSP0_HWINJ_STRAIN-1127687622_tapered-100.gwf V1:FAKE-STRAIN_INJ hoft 1. 1102809610 1600 TF_Flat

FDOUT_FILE V1-INSP0_HWINJ_STRAIN-1127687622_tapered_PCal_notch2300HzQ100_fmax3000 1000 "*STRAIN *Ca_PCal* *NOISE* *hoft*"

#-----output
FDOUT_FRAME_DURATION 1
FDOUT_COMPRESSION 9
FDOUT_CHPREFIX2 "V1:"

```

### C.4 Some more plots

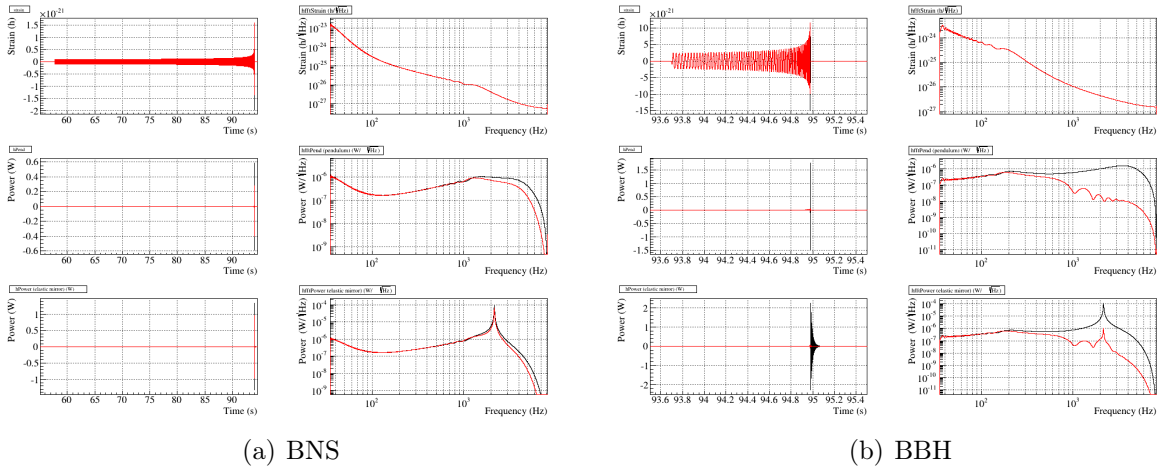
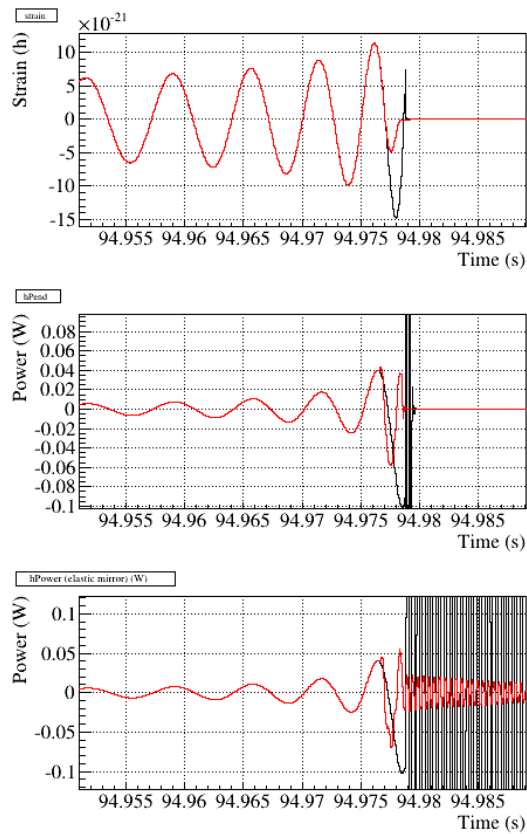


Figure 11: Example of the PCal laser power needed to inject a CBC signal (BNS or BBH) for a source located above the Virgo interferometer, at a distance of 20 Mpc. The figure 4 is a zoom of these time series around the last cycles of the CBC. For each figure, the first column shows the time series and the second column their FFTs (computed over 2 s windows). Two different simulations were done: with (red) or without (black) tapering of the end of the times series; top: time series of the simulated  $h(t)$  signals of the CBC. middle: time series of the derived power to be generated by the PCal in the case of a rigid mirror. bottom: time series of the derived power to be generated by the PCal in the case of an elastic mirror.





(a) BBH

Figure 12: Example of the PCal laser power needed to inject a CBC signal (BBH) for a source located above the Virgo interferometer, at a distance of 20 Mpc. It is the same as the BBH shown in figure 4 but zoomed in  $y$  around the tapered CBC signal (red). Two different simulations were done: with (red) or without (black) tapering of the end of the times series; top: time series of the simulated  $h(t)$  signals of the CBC. middle: time series of the derived power to be generated by the PCal in the case of a rigid mirror. bottom: time series of the derived power to be generated by the PCal in the case of an elastic mirror.